

DOI: 10.1002/celec.201300197

# Electrochemical Co-Deposition of Phosphonate-Modified Carbon Nanotubes and Tantalum on Nitinol

Anthony Maho,<sup>[a, b]</sup> Simon Detriche,<sup>[a]</sup> Grégory Fonder,<sup>[a]</sup> Joseph Delhalle,<sup>[a]</sup> and Zineb Mekhalif<sup>\*[a]</sup>

Nitinol substrates are coated with thin surface films made of carbon nanotubes (CNTs) and tantalum (Ta), with the aim of fostering their osseointegration aptitudes. Exceptional mechanical and chemical characteristics of CNTs combined with the resistance to corrosion and strong bioactive properties of tantalum allow for the generation of adherent, protective and functional layers on metallic biomaterial platforms. The composite coatings are elaborated on Nitinol through a two-step electrochemical protocol; firstly, through the electrophoretic deposi-

tion of phosphonate-modified CNTs and, secondly, with electrodeposition of Ta. As a preliminary step, phosphonate groups, acting, in addition, as specific Ta-capture entities, are introduced on the CNT sidewalls by means of diazonium derivatives, which imply no hard oxidative treatment. X-ray photoelectron spectroscopy as well as scanning and transmission electronic microscopies are used to analyse the chemical composition, structure and morphology of the different layers.

## 1. Introduction

Composite layers made of metals/ceramics and nanoparticles constitute recent promising developments in numerous nanomaterials and surface-treatment topics. Application fields stretch from the automobile industry to medical devices, aeronautics, electronics, sensors, energy storage and many others. The main processing techniques consist of powder metallurgy, thermal spraying, sol-gel and electrochemistry.<sup>[1–4]</sup>

This paper specifically features tantalum (Ta) and carbon nanotubes (CNTs) as components of hybrid thin films deposited on titanium-based substrates through an electrochemical process. The aim of the present study is to design robust, functional and biocompatible platform biomaterials for orthopaedic applications such as prosthesis and medical equipment. The base substrate is Nitinol (NiTi), an almost equiatomic nickel–titanium alloy, which is exploited here for its good biocompatibility and resistance to corrosion. Its mechanical characteristics of shape-memory, superelasticity and high-damping capacity are particularly sought after in the elaboration of flexible articular implants (shape-memory staples, spinal correctors, vertebral spacers, internal fixators for long bone shafts etc.). However, specific strategies are required to reduce the immune response, owing to the possible release of nickel-containing species in the human body, which can provoke allergenic and carcinogen effects over time, but also to consolidate the barrier-effect towards aggressive agents from the external environment.<sup>[5–9]</sup> With this perspective, a thin Ta coating is deposited

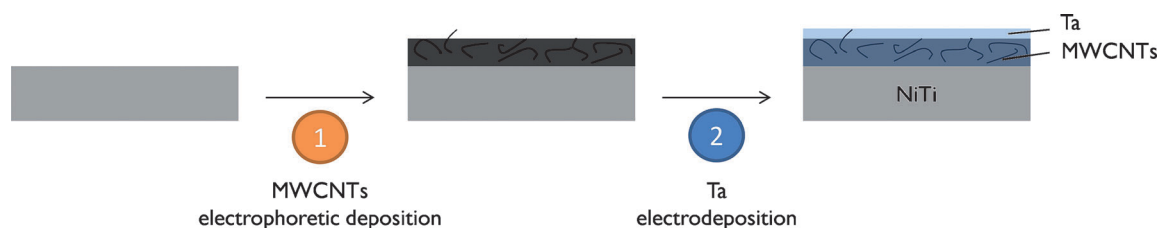
on the NiTi surface to increase chemical stability and protection towards corrosion, as well as to reinforce osseointegration and radio-opacity abilities.<sup>[10–12]</sup> In addition, the remarkable properties of multiwalled CNTs (MWCNTs) allow for their use as filling elements within a composite layer. Indeed, they have been proven to boost the (bio)chemical reactivity through the introduction of selected functional groups on the CNT sidewalls, to mechanically strengthen the surface layer, and to bring biomimetic elements with the collagen fibre structure.<sup>[1–3, 13]</sup>

The simultaneous electrochemical deposition of two constituents is somehow regarded as more complex than that of single one. Several experimental parameters, in terms of the solvent (polarity, electrochemical window, viscosity etc.) and/or the nanoparticles (nature, size, concentration, dispersion ability etc.), must be carefully and synergistically considered; their residual impact on surface morphology, mechanical resistance and chemical composition of the deposits are often of crucial importance.<sup>[4, 14–17]</sup> For these reasons, we consider a two-step experimental protocol (Scheme 1). First, an electrophoretic deposition (EPD) of chemically-modified MWCNTs on NiTi plates is performed; this fast and cost-effective technique involves simple equipment and is applicable to a large variety of materials.<sup>[17–20]</sup> This is followed by the electrodeposition (EDP) of Ta on the MWCNTs/NiTi substrates in an ionic-liquid solution, a method selected here for its practical ease and its high capacity of controlling the morphology, thickness and composition of the deposited material.<sup>[21, 22]</sup> It is also expected that the metallic coating electrodeposited on the surface achieves strong bonding between MWCNTs and Ta.

The present study involves the use of chemically modified MWCNTs. Such treatments are required for allowing the homogeneous and stable dispersion of the CNTs in the solvent used

[a] A. Maho, Dr. S. Detriche, Dr. G. Fonder, Prof. J. Delhalle, Prof. Z. Mekhalif  
Laboratory of Chemistry and Electrochemistry of Surfaces  
University of Namur, Rue de Bruxelles 61, 5000 Namur (Belgium)  
E-mail: zineb.mekhalif@unamur.be

[b] A. Maho  
Fonds pour la Formation à la Recherche dans l'Industrie et  
dans l'Agriculture, Rue d'Egmont 5, 1000 Bruxelles (Belgium)



**Scheme 1.** Preparation of 1) MWCNTs/NiTi samples through EPD and 2) Ta/MWCNTs/NiTi samples through EDP.

for their EPD on NiTi.<sup>[23–25]</sup> These functionalisations can also be considered as a direct way of introducing chemical functions on the CNT sidewalls, presenting a strong affinity for Ta entities during their EDP on MWCNTs/NiTi. The functional groups considered here contain of phosphonate ( $-\text{PO}_3\text{R}_2$ ) derivatives, given the high affinity of phosphonic acids for Ta.<sup>[26–28]</sup> Several reports have already described the covalent grafting of  $-\text{PO}_3\text{R}_2$  groups at the surface of CNTs,<sup>[29–32]</sup> among these, our recent paper has highlighted the direct binding of bisphosphonic acid functions on MWCNTs, with the introduction of two  $-\text{PO}_3\text{H}_2$  moieties per anchoring point, and the formation of strong covalent P–C–P bonds directly on the outer surface of the CNTs.<sup>[32]</sup> However, the synthesis protocol of such bisphosphonic-acid-modified CNTs resorts to oxidised carbon MWCNTs. Classically, such oxidative modifications result in shortened CNTs with lower aspect ratios, which can involve a partial loss of their mechanical resistance capacities, in particular when they are eventually included into composite coatings.<sup>[33]</sup> Therefore, we used another well-known method of MWCNTs functionalisation, which is clean and less aggressive (implying no oxidative treatments), through the covalent grafting of diazonium salts species, bearing  $-\text{PO}_3\text{Et}_2$  terminal functions in this case, onto CNTs sidewalls (Scheme 2).<sup>[34–36]</sup>

Elaboration of composite layers on titanium-based substrates for orthopaedic biomaterial perspectives is described and commented on hereafter. A two-step electrochemical process is considered, first with EPD of diethyl phosphonate-modified MWCNTs ( $\text{PO}_3\text{Et}_2$ -MWCNTs) on NiTi plates, then with Ta EDP on  $\text{PO}_3\text{Et}_2$ -MWCNTs/NiTi surfaces. Both processes constitute choice techniques of high precision for producing thin coatings from liquid solutions. The different layers and their

components are characterised by using X-ray photoelectron spectroscopy (XPS), scanning electron microscopy (SEM) and transmission electron microscopy (TEM).

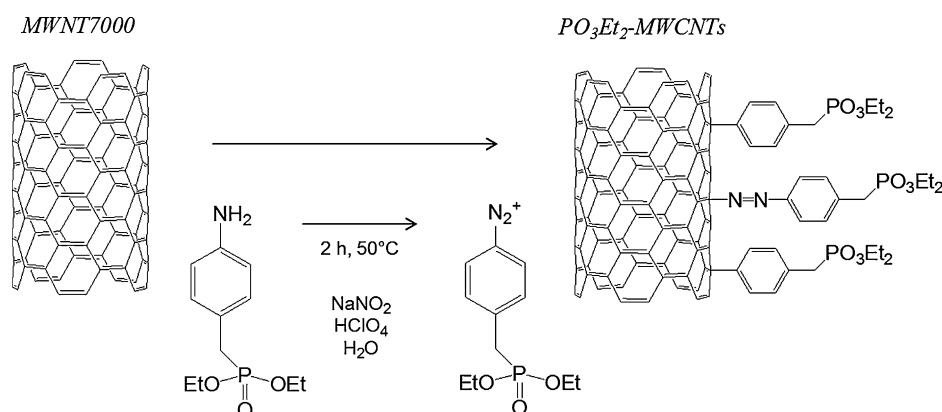
## 2. Results and Discussion

The initial stage of this study was devoted to the setting up of experimental parameters for the EPD of  $\text{PO}_3\text{Et}_2$ -MWCNTs on NiTi in aqueous solution. After preliminary trials (results not shown), a potential difference of 25 V and a deposition time of 1 min were determined as optimal values for obtaining thin, uniform and adherent layers. Following the deposition procedure, thermal post-treatment of the samples at 120 °C during 5 h was performed to reinforce the films compaction and toughness.

$\text{PO}_3\text{Et}_2$ -MWCNTs were first characterised through XPS analyses in order to validate the presence of the phosphonate functions on the CNT sidewalls. The representative survey spectrum of the CNTs powder, presented in Figure 1 a, exhibits an intense C1s peak, characteristic of CNTs and carbon atoms, which belong to the benzylphosphonate terminal functions.  $\text{PO}_3\text{Et}_2$  groups are also identified through P2p and O1s signals at respective binding energies ( $E_b$ ) of 133.5 and 532.5 eV. The probable occurrence of diazo links (Scheme 2), unreacted diazonium salt and/or residual aniline precursor is assessed by the N1s contribution at 400.4 eV.<sup>[35]</sup> Similar observations in terms of peaks existence and position are made for electrophoretically deposited  $\text{PO}_3\text{Et}_2$ -MWCNTs on NiTi (Figure 1 b), confirming their presence on the metallic substrates.

Global atomic percentages for both samples are presented in Table 1. Interestingly, P2p, N1s and O1s quantities slightly decrease from the MWCNTs powder to the EPD sample. It indicates that MWCNTs bearing quantitatively less  $\text{PO}_3\text{Et}_2$  functions are preferentially deposited on the NiTi surfaces.

This trend is confirmed by the further analysis of the C1s core level for both substrates. Figure 2a shows the corresponding spectra. Seven entries are identified: carbide-like species (traces) at 282.0 eV (1), C=C functionality from the MWCNTs and the corresponding shake-up satellite at 284.1 eV (2) and 290.4 eV (7), re-



**Scheme 2.** Functionalisation protocol of phosphonate-modified MWCNTs.

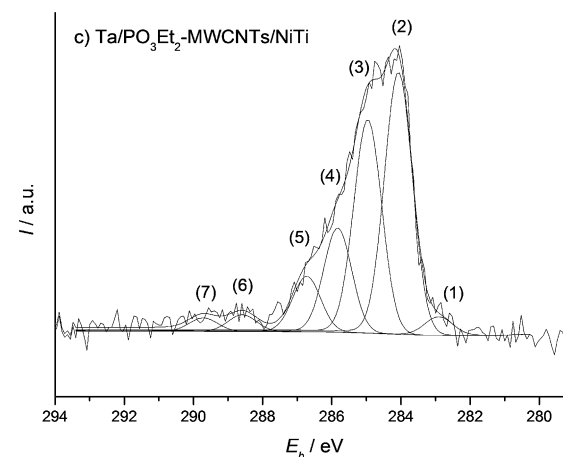
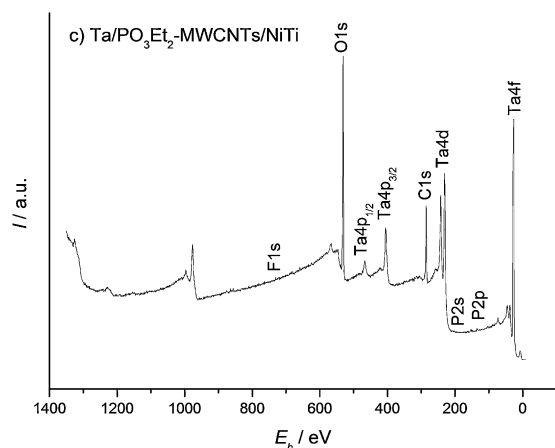
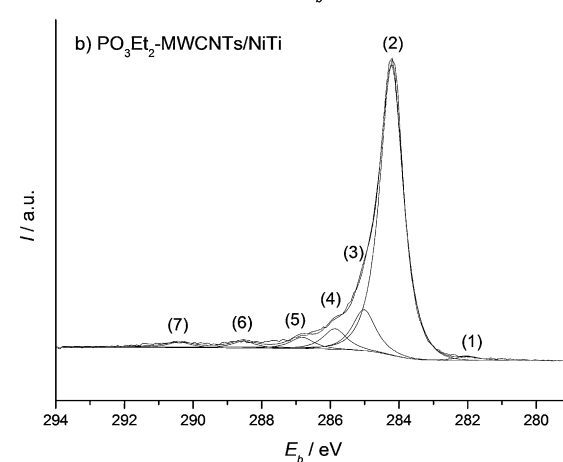
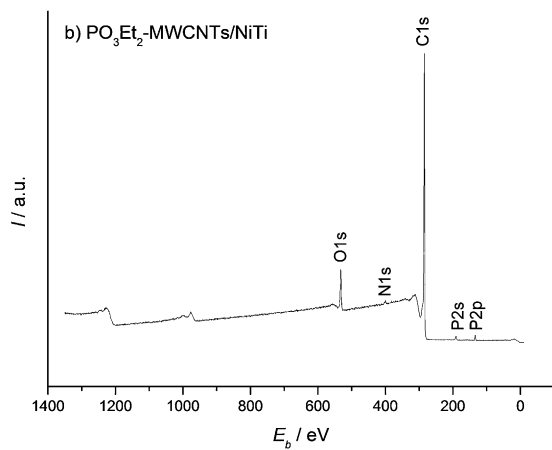
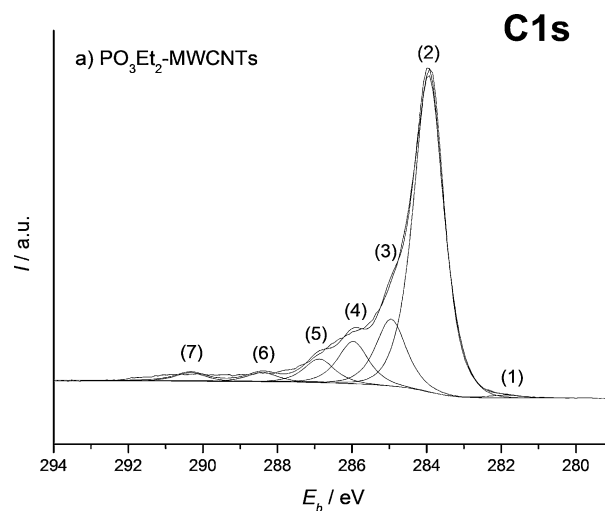
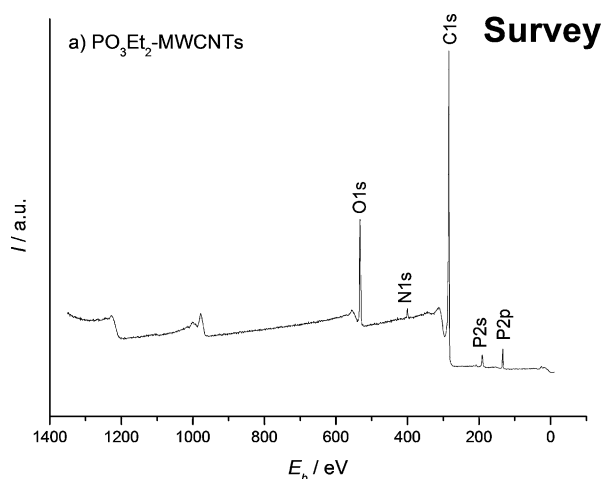


**Figure 1.** XPS survey spectra of a)  $\text{PO}_3\text{Et}_2$ -MWCNTs, b)  $\text{PO}_3\text{Et}_2$ -MWCNTs/NiTi and c) Ta/ $\text{PO}_3\text{Et}_2$ -MWCNTs/NiTi (with a Ta EDP time of 60 min).

**Figure 2.** XPS C 1s core level spectra of a)  $\text{PO}_3\text{Et}_2$ -MWCNTs, b)  $\text{PO}_3\text{Et}_2$ -MWCNTs/NiTi and c) Ta/ $\text{PO}_3\text{Et}_2$ -MWCNTs/NiTi (with a Ta EDP time of 60 min).

Substrate	Elemental composition [%]					
	C 1s	O 1s	P 2p	N 1s	Ta 4f	F 1s
$\text{PO}_3\text{Et}_2$ -MWCNTs	80.7	14.1	3.4	1.8	–	–
$\text{PO}_3\text{Et}_2$ -MWCNTs/NiTi	88.0	8.6	1.8	1.6	–	–
Ta/ $\text{PO}_3\text{Et}_2$ -MWCNTs/NiTi <sup>[a]</sup>	40.0	44.6	1.2	–	13.5	0.7

[a] With a Ta EDP time of 60 min.

spectively, C–C and C–H at 285.0 eV (3), C–N, C–O and C–P=O at 286.0 eV (4), C–P–O at 286.9 eV (5), as well as oxidised contaminations [classically C(=O)O] at 288.5 eV (6).<sup>[35,37–39]</sup> Table 2 details the atomic percentages of the different contributions. As observed with global atomic percentages (Table 1), contributions typical of  $\text{PO}_3\text{Et}_2$ -modified CNTs (peaks 3–5) are reduced after the EPD step. Also, percentages of the crude CNT contributions (peaks 2 and 7) increase, demonstrating the pres-

Table 2. XPS atomic percentages of the different contributions in the C 1s core-level signal.							
Substrate	Peak <sup>[a]</sup> [%]						
	(1)	(2)	(3)	(4)	(5)	(6)	(7)
PO <sub>3</sub> Et <sub>2</sub> -MWCNTs	0.6	66.2	15.0	8.9	5.0	2.6	1.7
PO <sub>3</sub> Et <sub>2</sub> -MWCNTs/NiTi	0.9	76.2	10.3	5.6	3.0	2.0	2.0
Ta/PO <sub>3</sub> Et <sub>2</sub> -MWCNTs/NiTi <sup>[b]</sup>	2.0	38.9	31.5	15.3	7.6	2.7	2.0

[a] (1) carbide, (2) C=C<sub>MWCNTs</sub>, (3) C-C, C-H, (4) C-N, C-O, C-P=O, (5) C=O, C-P-O, (6) C(=O)O, (7) shake-up or CO<sub>3</sub><sup>2-</sup>. [b] With a Ta EDP time of 60 min.

ence of quantitatively less PO<sub>3</sub>Et<sub>2</sub>-modified MWCNTs in the layer.

For Ta EDP on the PO<sub>3</sub>Et<sub>2</sub>-MWCNTs/NiTi surfaces, explorative experiments were first undertaken in order to determine the optimised practical conditions of deposition method and time. As noticed in previous studies,<sup>[40,41]</sup> the galvanostatic deposition process leads to better results in terms of Ta adherence, compared to cyclic voltammetry or potentiostatic deposition. A current-density value of  $-100 \mu\text{A cm}^{-2}$ , determined as optimal for the EDP of Ta on Ti and NiTi surfaces,<sup>[40,41]</sup> was again used here. A comparative study involving SEM and XPS measurements was then conducted to describe the evolution of the Ta EDP process over time. Morphological features of the Ta/PO<sub>3</sub>Et<sub>2</sub>-MWCNTs/NiTi samples were analysed by using SEM for 1, 30, 60 and 120 min durations, which were compared with their unchanged PO<sub>3</sub>Et<sub>2</sub>-MWCNTs/NiTi counterparts (Figure 3 a). The punctual apparition of the first nanometric Ta particles on the CNTs was noticed after only 1 min (red circles in Figure 3 b). Ta wrapping progressively increased after 30 min (Figure 3 c), with a granular but more uniform structure. The 60 min deposition time led to thicker and smoother Ta layers around the CNTs (Figure 3 d). Ultimately, the 120 min treatment (Figure 3 e) resulted in no further significant morphological changes, with a global aspect similar to the previous case.

The thickness values of the Ta films on the CNTs were estimated from SEM images of the uncoated (Figure 3 a) and coated (Figure 3 b–e) CNTs (red delimitations) and the data are reported in Table 3. The sporadic Ta deposits obtained after 1 min cannot be considered as genuine wrapping of the CNTs (quasi-zero experimental value); however, the average measurements obtained for longer durations are more consistent, increasing from 3.5 nm after 30 min to 5.0 nm after 60 min, and 6.0 nm after 120 min. The experimental ratios of

Table 3. Ta <sub>2</sub> O <sub>5</sub> layer thickness and XPS Ta/C=C <sub>MWCNTs</sub> and Ta/F ratios of the different Ta/PO <sub>3</sub> Et <sub>2</sub> -MWCNTs/NiTi substrates.			
EDP time [min]	Ta <sub>2</sub> O <sub>5</sub> layer thickness [nm]	Ta/C=C <sub>MWCNTs</sub>	Ta/F
1 min	≈ 0	0.02	2.0
30 min	3.5	0.12	4.3
60 min	5.0	0.85	21.2
120 min	6.0	1.07	6.7

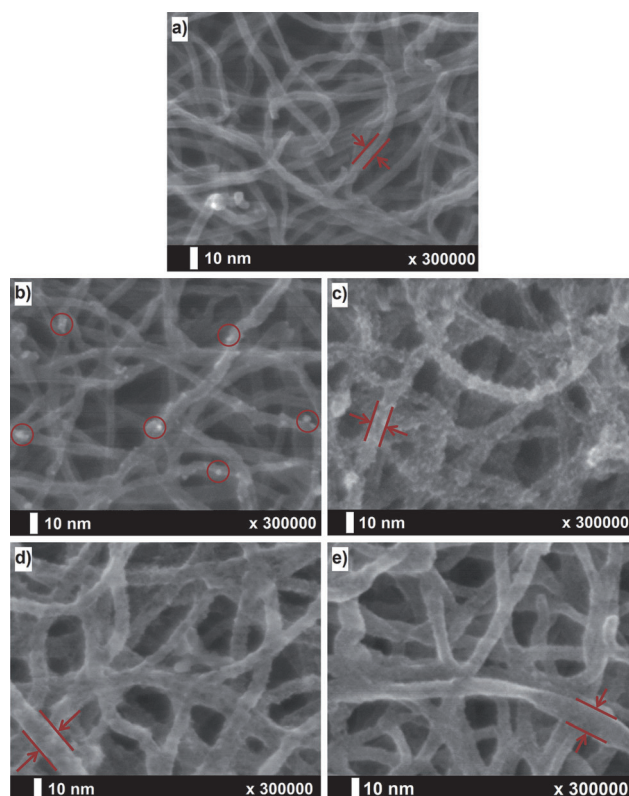


Figure 3. SEM images of PO<sub>3</sub>Et<sub>2</sub>-MWCNTs/NiTi (a) and Ta/PO<sub>3</sub>Et<sub>2</sub>-MWCNTs/NiTi samples after a Ta EDP time of 1 (b), 30 (c), 60 (d) and 120 min (e).

Ta/C=C<sub>MWCNTs</sub> (Table 3), which were obtained through XPS, further explain the increase in the quantity of Ta deposited on the CNTs with time; from a ratio of 0.02 after 1 min to 0.12 after 30 min, 0.85 after 60 min and 1.07 after 120 min. In parallel, the Ta/F ratios rise progressively up to 60 min (21.2) and then decrease abruptly after 120 min (6.7). This seems to be indicative of an overload behaviour, occurring for long EDP times (larger than 60 min), with a residual sorption of more TaF<sub>x</sub> (with  $x \leq 5$ ) contaminant species on the substrates. Such achievements, leading to F-enriched Ta layers, have to be avoided for biocompatibility reasons.<sup>[42]</sup>

The 60 min Ta EDP case can, thus, be endorsed as an optimum deposition method in terms of layer adherence, structure, thickness and number of fluorine contaminants. Detailed XPS characterisations are described in Figure 1 c (survey spectrum), Figure 2 c (C 1s core level), Table 1 (global atomic composition) and Table 2 (contributions of the C 1s signal). In addition to the residual C 1s, O 1s and P 2p signals testifying for the presence of the PO<sub>3</sub>Et<sub>2</sub>-MWCNTs, characteristic peaks of the Ta deposit (Ta 4f) and slight fluorine contaminations (F 1s) from the LiF additive are observed. The increase of aliphatic carbon proportions in the C 1s spectrum (Figure 2 a) at 285.0 eV (3), as well those of C-N and C-O at 285.8 eV (4), C=O at 286.7 eV (5), C(=O)O at 288.6 eV (6) and CO<sub>3</sub><sup>2-</sup> at 289.7 eV (7),<sup>[37,38]</sup> are attributed to further contamination inherent to the EDP process. Ta is detected in its oxidised form, Ta<sub>2</sub>O<sub>5</sub>, at 26.6 eV (Ta 4f<sub>7/2</sub> signal). The experimental O/Ta ratio is 3.3, with the theoretical value for Ta<sub>2</sub>O<sub>5</sub> being 2.5. The slight oxygen excess is, thus, at-

tributed to the oxygen atoms of the  $\text{PO}_3\text{Et}_2$  groups on the MWCNTs, and to inherent atmospheric contamination.

Pristine and Ta-covered  $\text{PO}_3\text{Et}_2$ -MWCNTs/NiTi substrates were also compared through SEM at different magnifications (Figure 4). The CNTs covered by a  $\text{Ta}_2(\text{O}_5)$  layer can be observed.

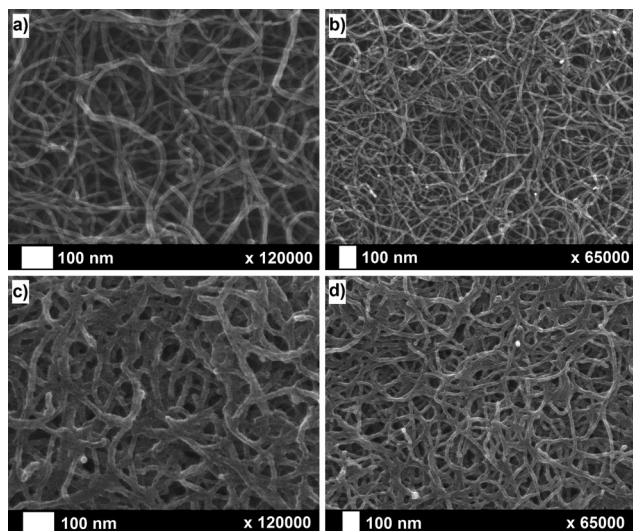


**Figure 4.** SEM pictures of a,b)  $\text{PO}_3\text{Et}_2$ -MWCNTs/NiTi and c,d) Ta/ $\text{PO}_3\text{Et}_2$ -MWCNTs/NiTi samples (with a Ta EDP time of 60 min).

In order to perform TEM analyses of both bare and Ta-modified- $\text{PO}_3\text{Et}_2$ -MWCNTs, the layers were scratched from the NiTi substrates and carefully dispersed in absolute ethanol, then a drop of the suspension was deposited on a TEM grid for characterisation.<sup>[32]</sup> Compared with their crude counterparts (Figure 5 a and b), the Ta-covered  $\text{PO}_3\text{Et}_2$ -MWCNTs (Figure 5 c and d) present strongly adherent and compact Ta aggregates over their entire outer surface.

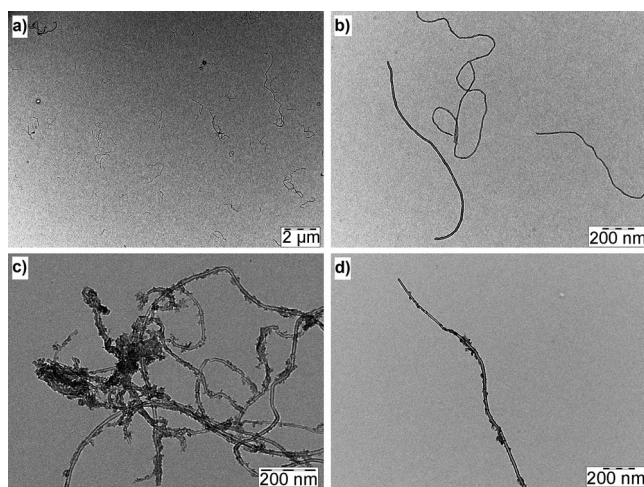


**Figure 5.** TEM pictures of a,b)  $\text{PO}_3\text{Et}_2$ -MWCNTs and c,d) Ta/ $\text{PO}_3\text{Et}_2$ -MWCNTs composite (with a Ta EDP time of 60 min) scratched from the NiTi surface.

### 3. Conclusions

The combination of the phosphonate-modified MWCNTs EPD and the Ta EDP processes leads to adherent, tough and homogeneous composite layers on NiTi plates. CNTs appear compactly and regularly deposited on the metallic surfaces. Their further modification with Ta leads to strong and uniform  $\text{Ta}_2\text{O}_5$ -wrapping, with a thickness of approximately 5 nm. Such hybrid surface films are, therefore, strongly believed to constitute choice platforms for further osseointegrative purposes. The occurrence of well-dispersed and uniformly Ta-covered CNTs at the direct interface between the NiTi biomaterial and the human body is expected to significantly improve mechanical and chemical interactions between the elements, and generate preferential sites for bone-cell adhesion and proliferation.

Additional experimental analyses and studies could complete and corroborate the first exploratory results presented here. Electrochemical characterisations at global (polarisation curves, impedance measurements) and local (scanning electrochemical microscopy) scales would bring useful and explicit data in connection with corrosion-protection issues. Extensive examinations of the mechanical features (stress testing) and bioactive aptitudes (hydroxyapatite growth, osteoblasts/osteoclasts colonisation) of the Ta/CNT composites would also assume particular importance for specific applied perspectives (work in progress).

More generally, concepts and methodologies developed in this work can be extended to other application fields of CNT functionalisation, deposition and/or decoration with metals. Main examples concern sensors (various biological molecules and chemical products), energy devices (fuel cells), as well as electrode and battery components (supercapacitors, semiconductors).<sup>[29,43–46]</sup> More specifically, the use of phosphonate-modified CNTs could also be of great interest for the generation of fire-resistant nanocomposite materials, as both phosphonic acid coupling molecules and jammed networks of CNTs are acknowledged for their flame-retardant capacities (notably into polymer matrices).<sup>[28,47]</sup>

### Experimental Section

#### Synthesis of $\text{PO}_3\text{Et}_2$ -MWCNTs

MWNT 7000 CNTs (0.240 g, Nanocyl) were mixed with diethyl 4-aminobenzylphosphonate (2.004 g, ABCR, 99%) and sodium nitrite (0.552 g, Sigma-Aldrich,  $\geq 99.0\%$ ) in ultra-pure water (120 mL,  $18.2 \text{ M}\Omega \text{ cm}$ ). Perchloric acid (828  $\mu\text{L}$ , Acros, 70%) was then added to the solution, which was stirred at  $50^\circ\text{C}$  for 2 h (Scheme 2). The samples were filtered and washed with distilled water, then dried for storage and further use.

#### NiTi Substrate Preparation

NiTi rectangular plates ( $20 \times 10 \times 0.3 \text{ mm}$ ) were purchased from AMF and constituted of Ni (56%) and Ti (balance). They were first mechanically polished on a Buehler EcoMet 300/AutoMet 250 instrument by using silicon carbide papers (P800 then P1200) and diamond pastes (9, 3, then  $1 \mu\text{m}$ ) purchased from Struers. NiTi coupons were then cleaned in absolute ethanol (VWR Prolabo) under

ultrasonication for 15 min, submitted to UV/ozone for 30 min (Jelight 42–220), and finally ultrasonically rinsed in absolute ethanol for a further 15 min, before being dried under nitrogen.

### EPD of PO<sub>3</sub>Et<sub>2</sub>–MWCNTs on NiTi

PO<sub>3</sub>Et<sub>2</sub>–MWCNTs (2.5 mg) were dispersed into ultra-pure water (15 mL) by using a Hielscher UP200S ultrasonic processor, and the resulting suspension was centrifuged in a Thermo Scientific Jouan B4i instrument for 30 min at 3000 rpm. The supernatant (10 mL) was then withdrawn as the working solution for the EPD experiments, which were carried out with a pre-treated NiTi plate as the anode and a platinum foil as the cathode. The two electrodes were placed parallel to each other, separated by 5 mm, and presented an area of contact with the CNTs dispersion of 1 cm<sup>2</sup>. A constant potential difference of 25 V was applied for 1 min, by using a Voltcraft VLP-2403 Pro DC power supply, to allow the migration of the CNTs towards the NiTi surface. The PO<sub>3</sub>Et<sub>2</sub>–MWCNTs/NiTi substrates were then carefully removed from the solution, and finally dried in an oven at 120 °C for 5 h.

### EPD of Ta on PO<sub>3</sub>Et<sub>2</sub>–MWCNTs/NiTi

The covering of PO<sub>3</sub>Et<sub>2</sub>–MWCNTs/NiTi substrates with an electrodeposited Ta coating was realised in an argon-filled glove box (residual quantities of water and oxygen below 30 ppm) by using an EG&G Princeton Applied Research Potentiostat/Galvanostat (Model 263 A). The working bath contained tantalum fluoride (0.10 M, Aldrich, 98%) and lithium fluoride (0.25 M, Sigma–Aldrich, ≥99%) in dry 1-butyl-1-methyl bis(trifluoromethylsulfonyl)imide ionic liquid ([BMP]Tf<sub>2</sub>N, IOLiTec, 99%). Ta EPD was performed in the galvanostatic mode at ambient temperature (25 °C); a constant current density of –100 μA cm<sup>–2</sup> was applied during a predefined time to the PO<sub>3</sub>Et<sub>2</sub>–MWCNTs/NiTi working electrode versus a platinum foil, acting as both reference and auxiliary electrodes. These were placed parallel to each other at a distance of 2 cm, and immersed in the experimental bath to achieve 1 cm<sup>2</sup> surface contact with the solution. The modified samples were post-treated by careful rinsing with acetone (Chem-Lab, 99+%), immersed for 15 min in boiling water, rinsed with absolute ethanol, and dried under nitrogen.

### XPS Characterisation

XPS spectra were measured on a Thermo Scientific K-Alpha spectrometer and treated by means of the Thermo Advantage v5.27 software. The photoelectrons were excited with monochromatic AlK<sub>α</sub> radiation as the excitation source, collected perpendicularly to the sample surface and detected with a hemispherical analyser. The spot size of the XPS source was 200 μm, and the analyser was operated with a pass energy of 150 eV for the survey spectra and 20 eV for the accumulation of spectra on core levels. Pressure was maintained below 1 × 10<sup>–8</sup> Torr during data collection. The binding energies of the obtained peaks were referenced to the C 1s signal of sp<sup>3</sup> carbon, which was set at 285.0 eV. Spectra were fitted with a smart background and a linear combination of Gaussian and Lorentzian profiles in 70:30 proportions. Peak positions were found to be approximately constant (±0.3 eV). The relative peak areas were estimated by using the following values for sensitivity factors: C 1s 1.000, O 1s 2.930, P 2p 1.192, N 1s 1.800, Ta 4f 8.620 and F 1s 4.430.

### SEM and TEM Imaging

JEOL 7500F and Phillips Tecnai 10 microscopes were used to obtain SEM and TEM images, respectively.

## Acknowledgements

A.M. is grateful to Fonds de la Recherche Scientifique (FNRS) for FRIA doctoral fellowship.

**Keywords:** electrochemistry · nanotubes · nitinol · phosphonate · tantalum

- [1] P. J. F. Harris, *Int. Mater. Rev.* **2004**, *49*, 31–43.
- [2] J. Cho, A. R. Boccaccini, M. S. P. Shaffer, *J. Mater. Sci.* **2009**, *44*, 1934–1951.
- [3] S. R. Bakshi, D. Lahiri, A. Agarwal, *Int. Mater. Rev.* **2010**, *55*, 41–64.
- [4] K. Jiang in *Cutting Edge Technology* (Ed.: D. Vasileksa), InTech, Rijeka, **2010**, pp. 391–412.
- [5] D. Mantovani, *JOM–J. Min. Met. Mater. S.* **2000**, *52*, 36–44.
- [6] S. A. Shabalovskaya, *Biomed. Mat. Eng.* **2002**, *12*, 69–109.
- [7] M. Geetha, A. K. Singh, R. Asokamani, A. K. Gogia, *Prog. Mater. Sci.* **2009**, *54*, 397–425.
- [8] M. H. Elahinia, M. Hashemi, M. Tabesh, S. B. Bhaduri, *Prog. Mater. Sci.* **2012**, *57*, 911–946.
- [9] L. De Nardo, L. Altomare, B. Del Curto, A. Cigada, L. Draghi in *Coatings for biomedical applications* (Ed.: M. Driver), Woodhead Publishing Limited, Cambridge, **2012**, pp. 106–142.
- [10] J. Black, *Clin. Mater.* **1994**, *16*, 167–173.
- [11] Y. Cheng, W. Cai, H. T. Li, Y. F. Zheng, *J. Mater. Sci.* **2006**, *41*, 4961–4964.
- [12] V. K. Balla, S. Bodhak, S. Bose, A. Bandyopadhyay, *Acta Biomater.* **2010**, *6*, 3349–3359.
- [13] S. Sirivisoot, T. J. Webster, *Nanotechnology* **2008**, *19*, 295101.
- [14] M. Musiani, *Electrochim. Acta* **2000**, *45*, 3397–3402.
- [15] C. T. J. Low, R. G. A. Wills, F. C. Walsh, *Surf. Coat. Technol.* **2006**, *201*, 371–383.
- [16] Y. Bai, M. P. Neupane, I. S. Park, M. H. Lee, T. S. Bae, F. Watari, M. Uo, *Mater. Sci. Eng. C* **2010**, *30*, 1043–1049.
- [17] M. F. De Riccardis, D. Carbone, V. Martina, M. Re, D. Meng, J. A. Roether, A. R. Boccaccini, *Key Eng. Mater.* **2009**, *412*, 87–92.
- [18] L. Besra, M. Liu, *Prog. Mater. Sci.* **2007**, *52*, 1–61.
- [19] A. R. Boccaccini, J. Cho, J. A. Roether, B. J. C. Thomas, E. J. Minay, M. S. P. Shaffer, *Carbon* **2006**, *44*, 3149–3160.
- [20] A. R. Boccaccini, C. Kaya, M. S. P. Shaffer in *Electrophoretic Deposition of Nanomaterials* (Eds.: J. H. Dickerson, A. R. Boccaccini), Springer, New York, **2012**, pp. 157–179.
- [21] L. P. Bicelli, B. Bozzini, C. Mele, L. D’Urzo, *Int. J. Electrochem. Sci.* **2008**, *3*, 356–408.
- [22] T. Schubert, S. Zein El Abedin, A. P. Abbott, K. J. McKenzie, K. S. Ryder, F. Endres in *Electrodeposition from Ionic Liquids* (Eds.: F. Endres, D. MacFarlane, A. Abbott), Wiley-VCH, Weinheim, **2008**, pp. 83–123.
- [23] D. Tasis, N. Tagmatarchis, A. Bianco, M. Prato, *Chem. Rev.* **2006**, *106*, 1105–1136.
- [24] Y.-P. Sun, K. Fu, Y. Lin, W. Huang, *Acc. Chem. Res.* **2002**, *35*, 1096–1104.
- [25] S. Detriche, J. B. Nagy, Z. Mekhalif, J. Delhalle, *J. Nanosci. Nanotechnol.* **2009**, *9*, 6015–6025.
- [26] D. Brovelli, G. Hähner, L. Ruiz, R. Hofer, G. Kraus, A. Waldner, J. Schlösser, P. Oroszlan, M. Ehrat, N. D. Spencer, *Langmuir* **1999**, *15*, 4324–4327.
- [27] E. Jaehne, S. Oberoi, H.-J. P. Adler, *Prog. Org. Coat.* **2008**, *61*, 211–223.
- [28] G. Guerrero, J. G. Alauzun, M. Granier, D. Laurencin, H. Mutin, *Dalton Trans.* **2013**, *42*, 12569–12585.
- [29] T. Sainsbury, D. Fitzmaurice, *Chem. Mater.* **2004**, *16*, 3780–3790.
- [30] B. Zhao, H. Hu, S. K. Mandal, R. C. Haddon, *Chem. Mater.* **2005**, *17*, 3235–3241.
- [31] A. Oki, L. Adams, V. Khabashesku, Y. Edigin, P. Biney, Z. Luo, *Mater. Lett.* **2008**, *62*, 918–922.
- [32] A. Maho, S. Detriche, J. Delhalle, Z. Mekhalif, *Mater. Sci. Eng. C* **2013**, *33*, 2686–2697.
- [33] V. Datsyuk, M. Kalyva, K. Papagelis, J. Parthenios, D. Tasis, A. Siokou, I. Kallitsis, C. Galiotis, *Carbon* **2008**, *46*, 833–840.
- [34] J. L. Bahr, J. M. Tour, *Chem. Mater.* **2001**, *13*, 3823–3824.
- [35] J. Y. Cai, J. Min, J. McDonnell, J. S. Church, C. D. Easton, W. Humphries, S. Lucas, A. L. Woodhead, *Carbon* **2012**, *50*, 4655–4662.

- [36] M. Raicopol, L. Necula, M. Ionita, L. Pitan, *Surf. Interface Anal.* **2012**, *44*, 1081–1085.
- [37] J. F. Moulder, W. F. Stickle, P. E. Sobol, K. D. Bomben in *Handbook of X-ray Photoelectron Spectroscopy* (Ed.: J. Chastain, J. F. Moulder), Perkin-Emmer Corporation, Eden Prairie, **1992**, pp. 33–195.
- [38] T. I. T. Okpalugo, P. Papakonstantinou, H. Murphy, J. McLaughlin, N. M. D. Brown, *Carbon* **2005**, *43*, 153–161.
- [39] I. Milošev, M. Metikos-Hukovic, Z. Petrovic, *Mater. Sci. Eng. C* **2012**, *32*, 2604–2616.
- [40] C. Arnould, J. Delhalle, Z. Mekhalif, *Electrochim. Acta* **2008**, *53*, 5632–5638.
- [41] A. Maho, J. Delhalle, Z. Mekhalif, *Electrochim. Acta* **2013**, *89*, 346–358.
- [42] L. Reclaru, J.-M. Meyer, *Biomaterials* **1998**, *19*, 85–92.
- [43] R. A. Guirado-Lopez, M. Sanchez, M. E. Rincon, *J. Phys. Chem. C* **2007**, *111*, 57–65.
- [44] G. Yang, L. Wang, J. Jia, D. Zhou, D. Li, *J. Solid State Electrochem.* **2012**, *16*, 2967–2977.
- [45] M.-C. Tsai, T.-K. Yeh, C.-H. Tsai, *Mater. Chem. Phys.* **2008**, *109*, 422–428.
- [46] J.-C. Kim, I.-S. Hwang, S.-D. Seo, D.-W. Kim, *Mater. Lett.* **2013**, *104*, 13–16.
- [47] T. Kashiwagi, F. Du, J. F. W. Douglas, K. I. Winey, R. H. Harris Jr., J. R. Shields, *Nat. Mater.* **2005**, *4*, 928–933.

---

Received: October 23, 2013

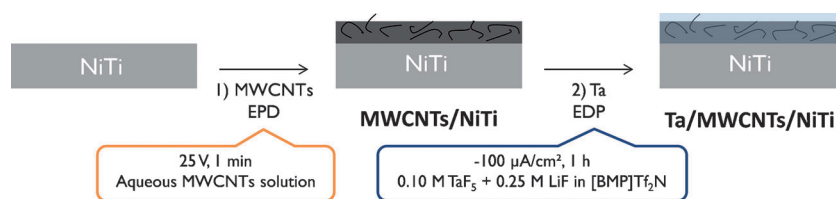
Published online on ■ ■ ■, 2014

## ARTICLES

A. Maho, S. Detriche, G. Fonder,  
J. Delhalle, Z. Mekhalif\*



### Electrochemical Co-Deposition of Phosphonate-Modified Carbon Nanotubes and Tantalum on Nitinol



**Bone idle:** Carbon nanotubes (CNTs) modified with phosphonate functions are electrophoretically deposited (EPD) on Nitinol (NiTi) plates. They are further coated with a thin tantalum electrodeposit (see picture). Such adherent and

functional surface layers are expected to reinforce mechanical and biochemical interactions with the human body within the framework of osseous implant integration and bone regeneration.